Development 126, 1055-1064 (1999)
Printed in Great Britain © The Company of Biologists Limited 1999
DEV5279

EGL-27 is similar to a metastasis-associated factor and controls cell polarity and cell migration in *C. elegans*

Michael A. Herman[1,3,*], QueeLim Ch'ng[2], Susan M. Hettenbach[1], Thomas M. Ratliff[1], Cynthia Kenyon[2] and Robert K. Herman[3]

[1]Division of Biology, Kansas State University, Manhattan, KS 66506, USA
[2]Department of Biochemistry and Biophysics, UCSF, San Francisco, CA 94143, USA
[3]Department of Genetics and Cell Biology, University of Minnesota, St Paul, MN 55108, USA
*Author for correspondence (e-mail: mherman@ksu.edu)

Accepted 17 December 1998; published on WWW 2 February 1999

SUMMARY

Mutations in the *C. elegans* gene *egl-27* cause defects in cell polarity and cell migration: the polarity of the asymmetric T cell division is disrupted and the descendants of the migratory QL neuroblast migrate incorrectly because they fail to express the Hox gene *mab-5*. Both of these processes are known to be controlled by Wnt pathways. Mosaic analysis indicates that *egl-27* function is required in the T cell for proper cell polarity. We cloned *egl-27* and discovered that a domain of the predicted EGL-27 protein has similarity to Mta1, a mammalian factor overexpressed in metastatic cells. Overlaps in the phenotypes of *egl-27* and Wnt pathway mutants suggest that the EGL-27 protein interacts with Wnt signaling pathways in *C. elegans*.

Key words: *Caenorhabditis elegans*, Cell polarity, Cell migration, LIN-44, EGL-27, EGL-20, Mta1, Wnt signaling

INTRODUCTION

The establishment of the body axes is among the first events to occur during animal development. For example, the dorsoventral axis of *Xenopus* embryos is determined by signals leading to the generation of the Spemann organizer (reviewed by Moon and Kimelman, 1998). The anteroposterior and dorsoventral axes of *Drosophila* embryos are determined by signaling between the oocyte and follicle cells leading to the generation of different cell fates along each axis (reviewed by Grunert and St Johnston, 1996). As these axes are established and cell fates are determined, cells must become oriented to each axis. This is particularly important for cells that divide asymmetrically to generate different daughter cells, where the relative orientation of the different daughter cells to each other and to the body axes gives each asymmetric division a polarity. For cells that migrate, orientation to the body axes may serve to guide them to their destinations. The mechanisms by which cell polarity and cell migration are controlled are not well understood.

In *C. elegans*, Wnt signaling pathways are important in controlling cell polarity and cell migrations. The Wnts are a conserved family of secretory glycoproteins that function as signaling molecules to control many different developmental processes (reviewed by Cadigan and Nusse, 1997). Genetic and molecular studies have determined the probable order of action of several components of a Wnt pathway affecting segment polarity in *Drosophila*: Porcupine (Porc) is required for the synthesis or secretion of the Wnt protein Wingless (Wg). Wg then acts through the Dfrizzled-2 (Dfz2) receptor (Bhanot et al., 1996). Inside the cell, Dishevelled protein is activated and antagonizes the action of Zeste-white 3 kinase (a homolog of glycogen synthase kinase 3), which results in the stabilization of Armadillo (a homolog of β-catenin) causing it to accumulate in the nucleus, where it appears to interact with Pangolin (a homolog of TCF/LEF-1) to activate transcription of target genes (Cadigan and Nusse, 1997). Components of this pathway have also been shown to function in dorsal axis formation in *Xenopus* (Moon et al., 1997), as well as in the development of mouse mammary tumors and human colon and skin carcinomas (Morin et al., 1997; Nusse and Varmus, 1982; Rubinfeld et al., 1997).

During *C. elegans* development, Wnt signaling controls the polarities of individual cells. MOM-2 is a Wnt signal produced in the four-cell embryo by the P_2 blastomere, which polarizes the EMS blastomere and thereby confers distinct fates on the EMS daughters: E, which generates endoderm, and MS, which gives rise to mesoderm (Rocheleau et al., 1997; Thorpe et al., 1997). Other components of the Wnt pathway also function in this process, including *mom-1*, a homolog of Porc, and *mom-5*, a member of the Frizzled (Fz) family. However, mutations affecting the TCF homolog POP-1 cause the opposite phenotype, suggesting that it represses signal transduction in the absence of Wnt signaling (Lin et al., 1995).

Wnt signaling also controls cell polarities in the tail of developing *C. elegans* larvae. Mutations in the *Wnt* gene *lin-44* cause the polarities of certain cells that divide asymmetrically in the tail of the animal – the B, TL and TR cells – to be reversed (Herman and Horvitz, 1994). LIN-44 is expressed in the epidermal cells at the tip of the tail, which are posterior to the

cells whose polarities are affected by *lin-44* mutations. Mosaic analysis has shown that *lin-44* functions in the same cells in which *lin-44* is expressed. These results suggested that LIN-44 is secreted by the epidermal cells at the tip of the tail and affects the polarity of asymmetric cell divisions that occur more anteriorly in the tail (Herman et al., 1995). Mutations in *lin-17*, which encodes a Frizzled-related protein (Sawa et al., 1996), lead to a loss of cell polarity (Sternberg and Horvitz, 1988) in the same cells in which *lin-44* mutations cause a reversal of cell polarity, suggesting that LIN-17 may be the receptor for LIN-44 signal. One model to explain the difference in phenotypes of mutations affecting a putative ligand (LIN-44) and receptor (LIN-17) is that there is a second signal, perhaps another Wnt, emanating from a source anterior to the B, TL and TR cells, which exerts an effect in the absence of LIN-44 (Sawa et al., 1996); there is as yet no evidence for such a signal, however.

Wnt signaling has also been shown to control certain cell migrations during *C. elegans* development. Mutations in the *Wnt* gene *egl-20* (Maloof et al., 1998) cause defects in the migrations of the HSN motor neurons, which drive the egg-laying muscles (Desai et al., 1988), and in migrations of the descendants of the QL neuroblast (Harris et al., 1996). The proper migration of the QL neuroblast descendants depends upon the expression and function of the Hox gene *mab-5* in the migrating cells (Kenyon, 1986; Salser and Kenyon, 1992), which in turn is dependent on *egl-20* function (Harris et al., 1996). Other components of the Wnt signaling pathway, including *lin-17* and a β-catenin-related protein encoded by *bar-1* (Eisenmann et al., 1998), also control the migrations of the QL descendants by regulating the expression of *mab-5* (Harris et al., 1996; Maloof et al., 1998).

We have found that mutations in *egl-27* lead to defects in TL and TR cell polarity, which are controlled by LIN-44 and LIN-17, as well as defects in the cell migrations of the two HSN cells and the QL neuroblast descendants, which are controlled by EGL-20, LIN-17 and BAR-1. We have cloned *egl-27* and found that it encodes a protein that contains a large domain resembling a metastasis-associated factor, Mta1 (Toh et al., 1994). We show that *egl-27* function is required in the TL and TR cells for normal cell polarity, suggesting that *egl-27* functions in the cells that receive Wnt signal. These results suggest that *egl-27* interacts with the Wnt pathway, perhaps by transducing the Wnt signal or another signal that functions in parallel to the Wnt pathway.

MATERIALS AND METHODS

General methods and strains

Nematodes were cultured by standard techniques (Sulston and Hodgkin, 1988). The following mutations were used: LGI, *unc-29(e1072)*; LGII, *dpy-10(e128), egl-27(n170, mn553, e2394, mn585), unc-4(e120), unc-52(e444), mnDf30, mnDf96, mnC1*; LG III, *mab-5(e1751gf)*; LG X, *mnIs7[lin-44::gfp; unc-29(+)]*.

Scoring of cell migrations

The QL.pa daughters were scored at the end of L1 as described by Harris et al. (1996). The positions of BDU, ALM, CAN and HSN were scored at hatching relative to the V and P cells.

Cell lineage analysis and T cell polarity

Living animals were observed using Nomarski optics; cell nomenclature and cell lineage analysis were according to Sulston and Horvitz (1977). An 'x' in the name of a cell is used to refer to both daughters of the cell name that appears before the 'x'. The divisions and migrations of Q cells derived from the Q/V5 cell were followed until late L1, when all the P cells had descended. The abnormal Q lineages were followed until cell migrations and divisions had ceased for >1 hour. Observations of the Q/V5 cell division in pretzel-stage embryos were started at least 2 hours prior to hatching and followed until hatching. Subsequent development of the Q/V5 lineage was observed from hatching to the formation of the postdeirid in late L2. Fates of the T cell descendants were determined by nuclear morphologies according to Herman and Horvitz (1994).

Phasmid dye-filling as an indicator of normal T cell polarity was scored as previously described (Herman and Horvitz, 1994).

Immunofluorescence with anti-MAB-5 antibodies

Staged young L1s (2-6 hours after hatching) were stained with anti-MAB-5 antibodies as described by Salser and Kenyon (1996). Defective MAB-5 expression in *egl-27* animals was observed in three independent staining experiments. MAB-5 staining in the QL.d cells was scored only in animals in which we observed MAB-5 staining in cells other than QL.d, such as V6 and P11/12.

Molecular analysis

Standard molecular biology methods (Sambrook et al., 1989) were followed, except where noted. The nucleotide sequence of genomic DNA through the *egl-27* locus was determined by the *C. elegans* Genome Consortium, and primers used were based on this sequence. The base pair numbers indicating the extents of PCR fragments used are relative to the C04A2 genomic sequence. Long PCR fragments used for transformation were generated from C04A2 using Expand Long Template PCR System (Boehringer Mannheim). The nucleotide sequences of both strands of the longest (2,589 bp) EST cDNA clone, yk1e2 (provided by Y. Kohara), were determined by MacConnell Research Corp. (San Diego, CA) using primers we provided. A 4.1 kb genomic PCR fragment extending over bp 1445-5588 was used to screen 4.2×10^6 clones from a λZAP cDNA library provided by R. Barstead and R. Waterston. We isolated five clones and determined (MacConnell) the nucleotide sequences of both strands of the longest (1,970 bp) of these, pSHC1, as well as the sequences of the ends of a 1.2 kb clone, pSHC2, which extends 5′ from pSHC1 and includes the last 9 nucleotides of the SL1 transpliced leader, AAGTTTGAG. Nucleotide sequencing showed that all but 27 bp of pSHC2 overlaps pSHC1 and that pSHC1 overlaps yk1e2 by 499 bp. The sequences of mutant alleles were determined from PCR-amplified genomic DNA. Southern blot analysis of *n170* genomic DNA probed with both C04A2 and F31E8 suggested that the left endpoint of *n170* is within a 6.5 kb *Hin*dIII fragment detected by F31E8, which overlaps C04A2 in sequence. *n170* deleted about 10 kb of DNA detected by C04A2. From *n170* genomic DNA, we were able to amplify a 1.1 kb fragment extending over bp 9670-10786, but not a 2.1 kb fragment extending over bp 8721-10786, indicating that the right endpoint of *n170* lies between base pairs 8721 and 9670 of C04A2. Identity of the 1.1 kb fragment was confirmed by sequence analysis. No other sequence changes in *n170* genomic DNA were detected.

Transgenic animals

DNAs were microinjected into the mitotic germline of hermaphrodites (Mello and Fire, 1995). For rescue experiments, pRF4, a plasmid containing the semidominant *rol-6(su1006)* allele, was coinjected to identify transgenic (roller) lines. We injected 20-50 μg/ml of the gel-purified long PCR fragments derived from C04A2, along with 50 μg/ml each of circular and linearized pRF4. We scored each line for phasmid dye-filling (Herman and Horvitz, 1994).

Expression experiments

A translational *egl-27::gfp* fusion that placed the GFP coding sequence and the *unc-54* 3′ UTR at the end of the EGL-27 coding sequence was constructed by PCR using C04A2 and GFP expression vector pPD95.75

(from A. Fire). The junction of the gel-purified recombinant PCR GFP construct was confirmed by sequence analysis, and the fragment was used for microinjection. The cosmid C45D10 contains *unc-29*(+) (Lackner et al., 1994) and was used as a coinjectable marker. Transgenic lines containing extrachromosomal arrays of the fusion construct and C45D10 were generated in the *unc-29* background. *mhEx7* is a transgenic array containing the *egl-27::gfp* fusion and C45D10 that rescues the phasmid dye-filling defect of both *mn553* and *n170* alleles.

Mosaic analysis

A strain of genotype *unc-29 I; egl-27(mn553) II* was used to generate *egl-27* mosaic animals. The polarity of the T cell was assessed in L1 animals by the nuclear morphologies of the T.xx cells and in L2, L3 and L4 animals by the positions of the phasmid socket cells PHso1L/R (TL/R.paa) and PHso2L/R (TL/R.pap) (Herman and Horvitz, 1994). The *egl-27::gfp* fusion gene rescued the T cell polarity defect and was expressed in every somatic nucleus scored; it was used both as a source of *egl-27*(+) function and as a cell-autonomous marker. We scored non-Unc L1 progeny descended from animals of genotype *unc-29; egl-27(mn553); mhEx7* for T cell polarities. We then used GFP expression to determine whether the T.xx cells contained the array and were GFP positive. If the array was missing from the T.xx cells, we scored a representative set of cells derived from all parts of the lineage to determine at which division the array was lost. Many mosaic animals also lost the extrachromosomal array at divisions of cells unrelated to TL and TR; however, the positions of these additional losses among the mosaic animals did not correlate with the loss of T cell polarity. Both the T cell polarity and positions of array loss were confirmed when the animals reached the L3 or L4 stage.

RESULTS

egl-27 mutants display defects in T cell polarity

In wild-type hermaphrodites the bilaterally symmetric T cells divide asymmetrically during the early L1 stage: T.a generates four hypodermal cells and one neuron whereas T.p generates five neural cells (Fig. 1). In *lin-44* mutants the polarity of the divisions of the T cell lineage is reversed: T.a generates five neural cells and T.p generates four hypodermal cells and one neuron (Herman and Horvitz, 1994). In *lin-17* mutants the polarity of the division of the T cell lineage is lost: both T.a and T.p generate hypodermal cells. The defects in T cell polarity observed in both *lin-17* and *lin-44* mutants cause the two neurons of the phasmid, a sensory structure in the tail, to fail to fill with fluorescent dyes (Herman and Horvitz, 1994; Herman et al., 1995; Sawa et al., 1996). To identify genes that might interact with *lin-17* and *lin-44* in the control of T cell polarity we screened for additional mutations that result in a phasmid dye-filling defect caused by defects in T cell polarity (M. A. H., C. Kari, and R. K. H., unpublished). Two of the new mutations isolated in this screen were alleles of *egl-27*, a gene originally identified in a screen for egg-laying defective (Egl) mutants (Trent et al., 1983). One of these, *egl-27(mn553)*, had a highly penetrant phasmid dye-filling defect, while the other, *egl-27(mn585)*, had a less severe defect (Table 1). Two previously identified *egl-27* mutations, *n170* and *e2394*

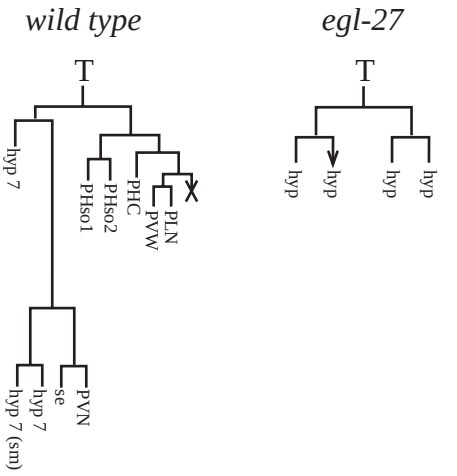

Fig. 1. Cell lineages of the T cell in wild-type and *egl-27* hermaphrodites. Wild-type hermaphrodite T cell lineage is shown on the left. The fates of many different cells in this lineage can be distinguished by nuclear morphology using DIC microscopy (Sulston and Horvitz, 1977; Herman and Horvitz, 1994). The hyp7 cells T.aa, T.apaa and T.apap join the hypodermal syncytium, but T.apaa has a smaller nucleus and is designated hyp7(sm). PHso1, PHso2, PVW, PHC and PLN, have similar nuclear morphologies. × indicates apoptosis. The seam cell (se) is a specialized hypodermal cell. We analyzed T cells lineages in six *mn553*, two *n170* and four *e2394* mutants, and all gave the pattern shown on the right. Each cell produced a non-specialized hypodermal nuclear morphology, designated hyp. T.ap frequently divided to generate 2-4 hypodermal descendants, indicated by the arrow. Specifically, T.ap: did not divide in one *mn553* animal, generated two hypodermal cells in two *mn553* animals, generated three hypodermal cells in one *mn553* and four *e2394* animals, and generated four hypodermal cells in two *n170* and two *mn553* animals.

Table 1. Penetrance of *egl-27* defects

Genotype	Phasmid dye-filling (%)	Embryonic and L1 arrest (%)	Presence of QL cells (%)	Presence of QR cells (%)
wild type	98 (*n*=472)	0 (*n*=314)	100 (*n*>100)*	100 (*n*>100)*
mn553	0 (*n*=356)	65 (*n*=349)	37 (*n*=152)	40 (*n*=161)
n170	0 (*n*=270)	46 (*n*=163)	54 (*n*=82)	52 (*n*=82)
e2394	0 (*n*=204)	11 (*n*=96)	64 (*n*=84)	63 (*n*=82)
mn585	27 (*n*=264)	68 (*n*=302)	ND	ND

Phasmid dye-filling was used as an indicator of normal T cell polarity (Herman and Horvitz, 1994). There is one phasmid on each side of the animal. n, number of sides of animals scored.

% lethality was scored as the proportion of animals at the L2 stage or older that had developed in 2 days from a known number of eggs that had been picked to fresh plates. During this time, arrested L1 larvae were observed but could not be accurately counted because they appeared sick and transparent and were easily missed in the dissecting microscope. *n*, number of eggs deposited on the plate at the beginning of the assay.

ND, not determined.

Presence of QL and QR was scored at hatching. *n*, number of sides of animals scored.

*Kenyon Laboratory, unpublished data.

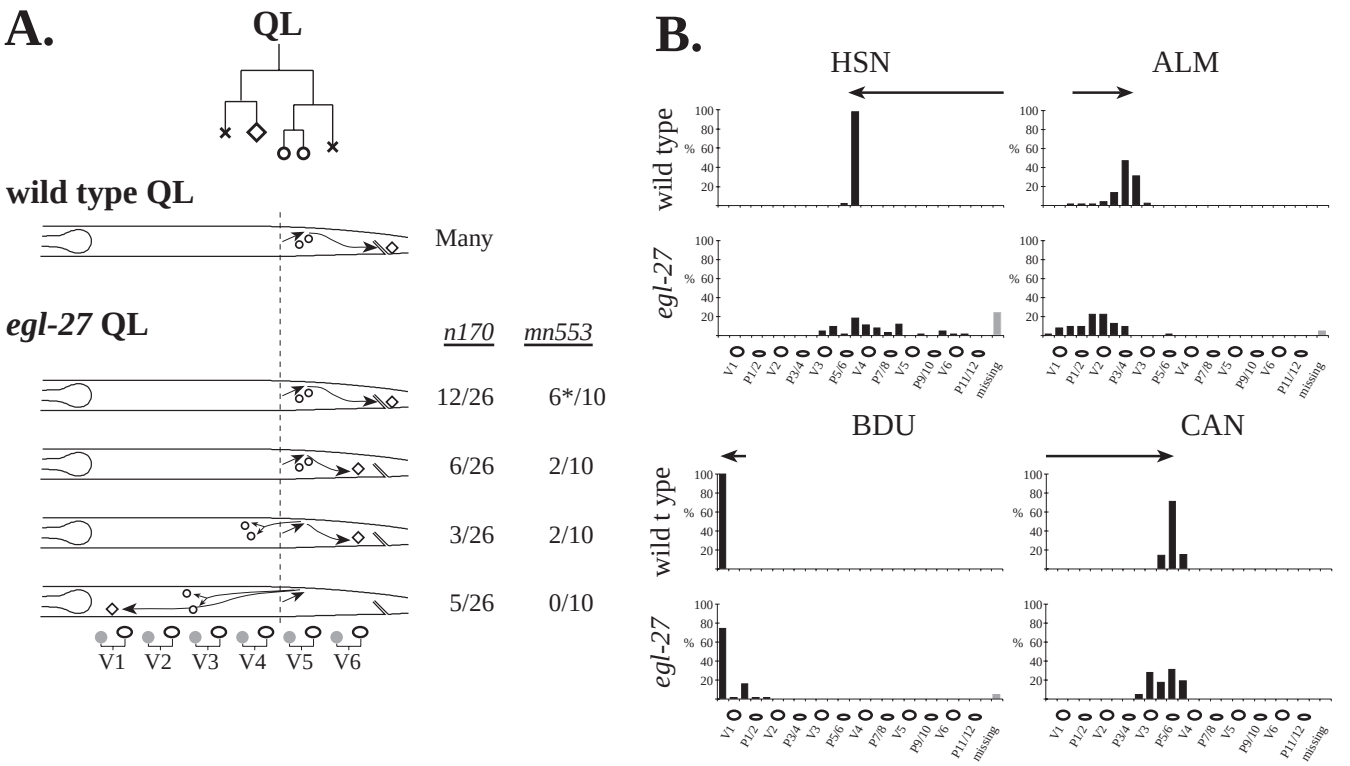

Fig. 2. Cell migration defects in *egl-27* mutants. (A) See text for description of QL descendant migrations in wild-type animals. QL cell descendant migration was analyzed only in animals where QL was present at hatching and gave rise to normal division patterns. Wild-type lineages of QL descendants are shown. × indicates apoptosis. Anterior is to the left. Dashed lines indicate the initial position of QL. Circles indicate the final positions of QL.paa (PVM) and QL.pap (SDQL), diamonds indicate the final positions of QL.ap (PQR). The extent of migration was judged by cell position relative to Vn.x cell positions (shown below each set of diagrams). Numbers indicate proportion of either *egl-27(mn553)* and *egl-27(n170)* animals in each category. * In one *mn553* animal QL.pp did not apoptose, which occurs at a low frequency in wild-type animals (Sulston and Horvitz, 1977). (B) HSN, ALM, BDU and CAN neuron cell migration in wild-type and *egl-27* animals. Arrows above each set of histograms indicate direction and extent of wild-type migrations. Cells were scored at hatching; their positions relative to the V and P cells present on the lateral side of the newborn L1 are indicated. Black bars indicate the proportion of cells at each position. Gray bars indicate the proportion of missing cells.

(A. Chisholm, personal communication), also cause defects in phasmid dye-filling (Table 1). Analysis of the T cell lineages of *mn553*, *n170* and *e2394* mutants showed that all have lost T cell polarity (Fig. 1).

egl-27 mutants display defects in the migrations of the QL descendants and other cells

The migratory neuroblasts QL and QR are left/right homologs that divide identically to give rise to three neurons and two cells that undergo apoptosis. Interestingly, the migrations of these cells and their descendants are left/right asymmetric. The QR neuroblast and its descendants migrate anteriorly. In contrast, the QL neuroblast migrates posteriorly and divides. The posterior daughter, QL.p, stops migrating and generates two neurons, PVM and SDQL, and a cell that undergoes apoptosis. The anterior daughter, QL.a, continues a posterior migration and divides to generate a cell that undergoes apoptosis and PQR, which continues to migrate posteriorly until it reaches its characteristic position in the tail (Fig. 2A) (Sulston and Horvitz, 1977). *egl-27* was previously reported to have misplaced QL descendants (denoted collectively as QL.d), suggesting a defect in these migrations (Hedgecock et al., 1987). On closer examination, we found that QL and QR were missing in some animals. This appeared to be caused by abnormalities in the divisions of AB.plapapaa (QL/V5L), the mother of QL and V5L, and in the divisions of AB.prapapaa (QR/V5R), the mother of QR and V5R (see below). To reduce the likelihood that the abnormal QL.d migrations of *egl-27* mutants were caused by misspecification of cell fate, we analyzed the migrations of these cells only in animals in which the QL cell lineages were normal. Furthermore, we found that when QL.paa (PVM) and QR.paa (AVM) were present, they expressed a *mec-7::GFP* reporter whose expression is generally limited to only six differentiated cells in the animal, including PVM and AVM. This suggests that the abnormal migrations of QL.d were not caused by misspecification of cell fate.

In *egl-27* animals with normal QL lineages, the QL neuroblast migrated posteriorly, as in wild-type animals, but the QL.d often migrated anteriorly (Fig. 2A). This phenotype is similar to that of *mab-5* loss-of-function mutants where the QL.d cells migrate anteriorly, mimicking the normal anterior migration of the QR descendants (denoted collectively as QR.d) (Kenyon, 1986; Salser and Kenyon, 1992). Thus, we asked if this defect could be due to an inability of the QL.d cells to turn on *mab-5*. We stained *egl-27* animals with antibodies to MAB-5 and observed a variable defect in MAB-5 expression in the QL.d cells of *egl-27(n170)* animals (Fig. 3A), consistent with the variability in the QL.d migration defect (Fig. 2A).

In *mab-5* gain-of-function (gf) mutants, which ectopically express *mab-5* (Hedgecock et al., 1987; Salser and Kenyon, 1992), both QL.d and QR.d cells migrate posteriorly, just as QL.d cells do in wild-type animals. The *egl-27* QL.d migration defect was corrected in an *egl-27*; *mab-5(gf)* double mutant: the QL.d cells migrated posteriorly (Fig. 3B), indicating that the QL.d migration defect in *egl-27* mutants is at least partially due to a lack of *mab-5* function and that *egl-27* controls *mab-5* expression in the QL.d cells. The cause of the incomplete penetrance of the QL migration and MAB-5 expression defects could be that none of the *egl-27* alleles examined are null; perhaps complete loss of *egl-27* function in QL would result in a fully penetrant defect.

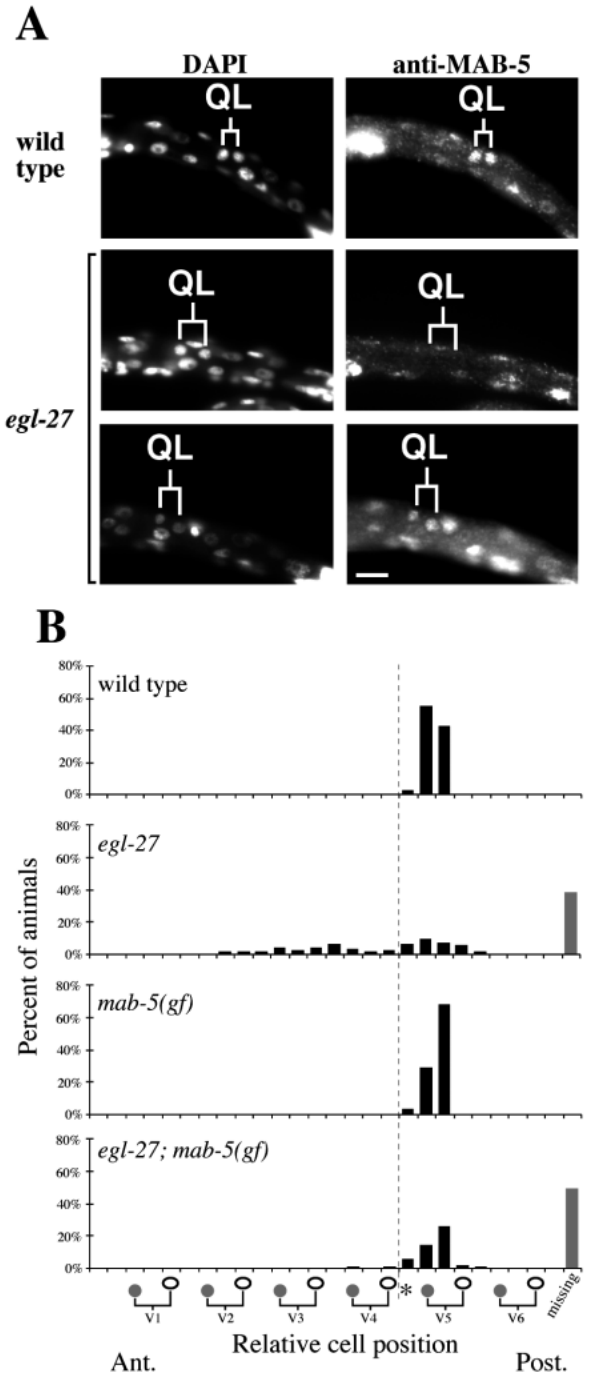

It was shown previously that in *egl-27* mutants, the two HSN motor neurons often fail to complete their embryonic migration from the tail of the animal where they are born to their final position in the mid-body (Desai et al., 1988). We have also observed abnormal migrations of the ALM, BDU and CAN neurons in *egl-27* mutants (Fig. 2B).

The Q/V5 precursors can divide abnormally in *egl-27* mutants

The QL and QR neuroblasts appeared to be missing in 25-50% of *egl-27* mutants, depending on the allele examined (Table 1). To infer the basis of this defect, we examined the cell divisions of their precursors, Q/V5L and Q/V5R (denoted collectively as Q/V5), in *egl-27* embryos. We found that Q/V5L failed to divide in 2/3 *mn553* embryos and 4/6 *n170* embryos and that Q/V5R failed to divide in 2/3 *mn553* embryos and 3/6 *n170* embryos. This accounts for the missing Q cells. In six *mn553* animals in which we inferred that Q/V5 divided normally (by the presence of Q at hatching), the postembryonic divisions of the Q and V5 lineages were normal (data not shown). However, when Q/V5 did not divide in the embryo (inferred by the absence of Q at hatching), Q/V5 divided abnormally after hatching. In two cases for *n170* and two for *mn553*, Q/V5 generated a cell lineage pattern similar to V5, as if Q/V5 were transformed to a V5-like cell. In two cases for *n170* and six for *mn553*, the Q/V5 division pattern was not similar to that of either Q or V5 alone but retained characteristics of each (data not shown), as if Q/V5 were transformed to a hybrid fate between Q and V5.

egl-27 mutants display embryonic and larval arrest

Homozygous *egl-27* mutants exhibit varying degrees of lethality, with *mn553* and *mn585* mutations the most and *e2394* the least severely affected (Table 1). The inviability was scored as both eggs that failed to hatch and L1 larvae that stopped developing. We crossed each *egl-27* mutant allele into a strain containing a genetically marked deficiency of the *egl-27* locus; that is, *egl-27 unc-4/+ +* males were crossed to *mnDf30 unc-4/mnC1[dpy-10 unc-52]* hermaphrodites, and Unc non-Dpy cross progeny (*egl-27 unc-4/mnDf30 unc-4*) were sought. *mnDf30* uncovers *dpy-10*; thus *mnDf30 unc-4/mnC1[dpy-10 unc-52]* hermaphrodites are Dpy, which allowed self and cross progeny to be distinguished. For each of the *egl-27* alleles we observed non-Unc non-Dpy cross progeny (*egl-27 unc-*

Fig. 3. *egl-27* controls the expression of MAB-5 in the QL.d cells. (A) MAB-5 expression in QL.a and QL.p. Whole-mount larvae, 3-6 hours post-hatching, were stained with polyclonal anti-MAB-5 antisera and the DNA stain DAPI (Salser et al., 1993). In wild-type animals (top panels) QL has just divided and both daughters stain brightly with anti-MAB-5 antisera (n>30). In many *egl-27* animals QL.a and QL.p did not stain with anti-MAB-5 antisera (center panels), while in others they did (bottom panels). Bar, 10 μm. (B) *mab-5(gf)* suppresses the anterior migrations of the QL.d cells in *egl-27* mutants. Final positions of the QL.pa daughters were scored (Harris et al., 1996) in wild-type (n=60), *egl-27(n170)* (n=183), *mab-5(e1751gf)* (n=59) single and *egl-27(n170); mab-5(e1751gf)* (n=117) double mutant animals. QL lineages were not determined; thus some of the QL.pa daughters scored were derived from abnormal QL lineages. The asterisk above V5.a marks the birthplace of QL. The dashed line marks the anteriormost position of QL.pax in wild-type animals. Black bars indicate the proportion of cells at each position. Gray bars indicate the proportion of missing cells.

4/mnC1, *mnDf30/+ +* and *mnC1/+ +*) but no *egl-27 unc-4/mnDf30 unc-4* Unc non-Dpy cross progeny, indicating that each of the *egl-27* alleles is 100% lethal when heterozygous with a deficiency of the locus. Control crosses in which *unc-4/+* males were crossed to *mnDf30 unc-4/mnC1[dpy-10 unc-52]* hermaphrodites produced both non-Unc non-Dpy and Unc non-Dpy cross progeny. We obtained identical results in a similar experiment using another deficiency of the locus, *mnDf96*. We observed arrested L1 animals on the cross plates in all cases. For each cross several Unc L1 larvae were picked and examined the next day to confirm that they were arrested. These data suggest that the existing *egl-27* mutations are not null and that *egl-27* may play roles in development in addition to controlling cell migrations and cell polarity.

Molecular cloning of *egl-27*

egl-27 maps genetically between *dpy-10* and *tra-2* on linkage group II (A. Chisholm, unpublished). We cloned *egl-27* by microinjecting cosmids and cosmid fragments into *egl-27* mutants and testing the transgenic animals for rescue of the T cell polarity defect. Microinjection of either cosmid C04A2 or a 16,738 bp PCR fragment derived from C04A2 rescued the T cell polarity defect (Fig. 4A). Overlapping cDNA clones specific to the rescuing region were identified from a collection of expressed

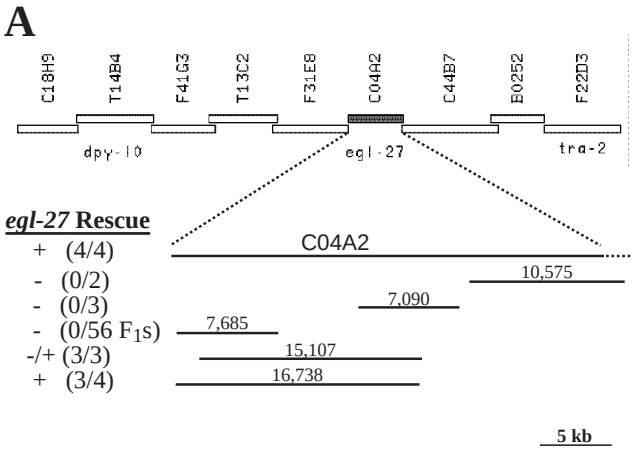

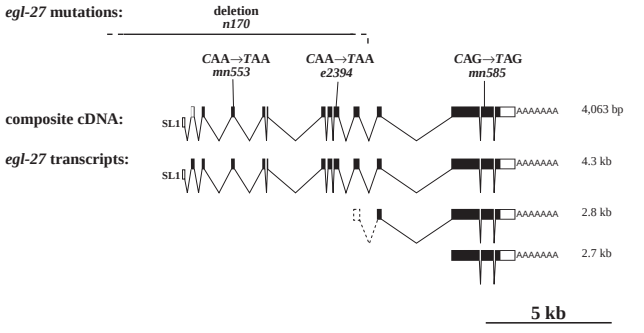

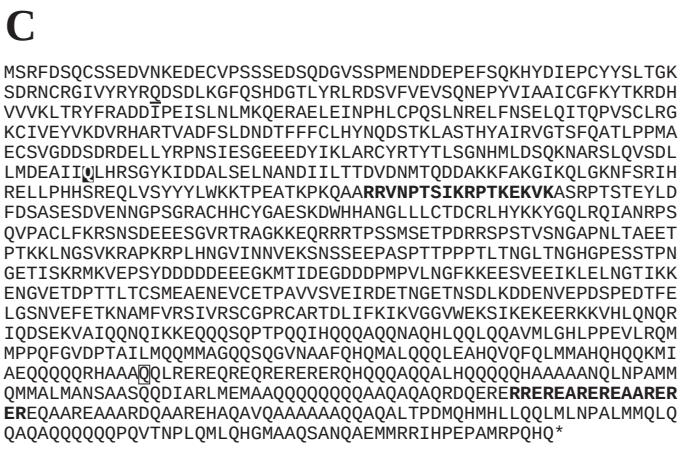

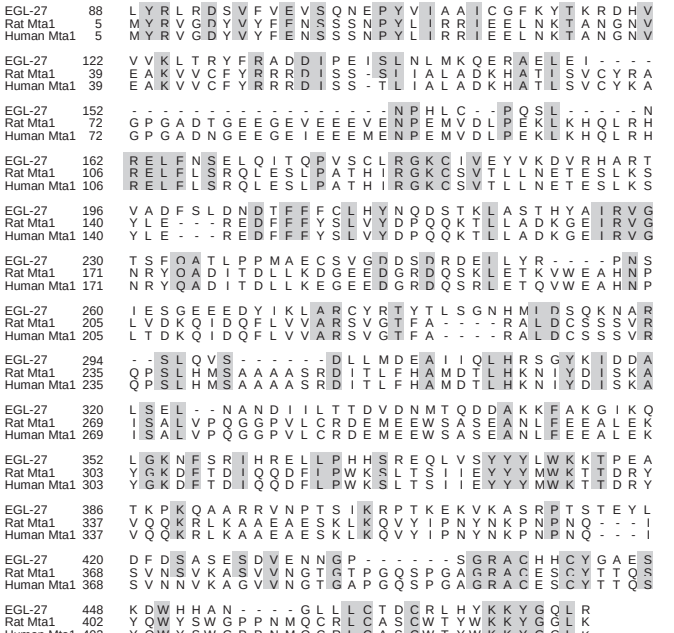

Fig. 4. Molecular cloning and analysis of the *egl-27* locus. (A) (Top) Physical map of sequenced cosmids in the region between *dpy-10* and *tra-2*. Only the unique portion of each overlapping cosmid is shown. Only C04A2 rescued *egl-27* mutants in microinjection experiments. (Bottom) Rescue data for C04A2 and PCR fragments derived from C04A2. Size (in bp) of each fragment is indicated. The number of lines rescued for the phasmid defect per total number of transgenic roller lines is given. We did not obtain any transgenic lines with the 7685 bp fragment, but we did examine 56 F_1 Roller animals, none of which were rescued. +, >85% of the transgenic animals were rescued; –/+, <40% of the transgenic animals were rescued; –, no rescue. (B) Molecular map of the *egl-27* locus and location of mutant lesions. Sequence analysis of C04A2 and the 4,063 bp composite cDNA revealed the intron/exon structure shown. Boxes indicate exons; closed portions indicate the open reading frame. Positions of the trans-spliced leader sequence, SL1, and the poly(A) tail are shown. The extents of the *n170* deletion and the positions of the base changes in the *mn553*, *e2394* and *mn585* point mutants are indicated. Schematics of the extents of the three *egl-27* transcripts as determined by northern analysis (Fig. 5) are also shown. The 2.8 kb transcript may begin in exon 9, indicated by the dotted line. (C) Predicted peptide sequence of EGL-27 with the bipartite nuclear localization sequences (bold), glutamine residues changed to stops in *mn553* (underlined), *e2394* (black box) and *mn585* (outlined box), indicated. (D) Alignment of the amino-terminal domain of EGL-27 with similar regions of the rat and human Mta1 proteins (Toh et al., 1995). Shaded boxes indicate identical residues. Line numbers indicate the residue number of the amino acid for each protein.

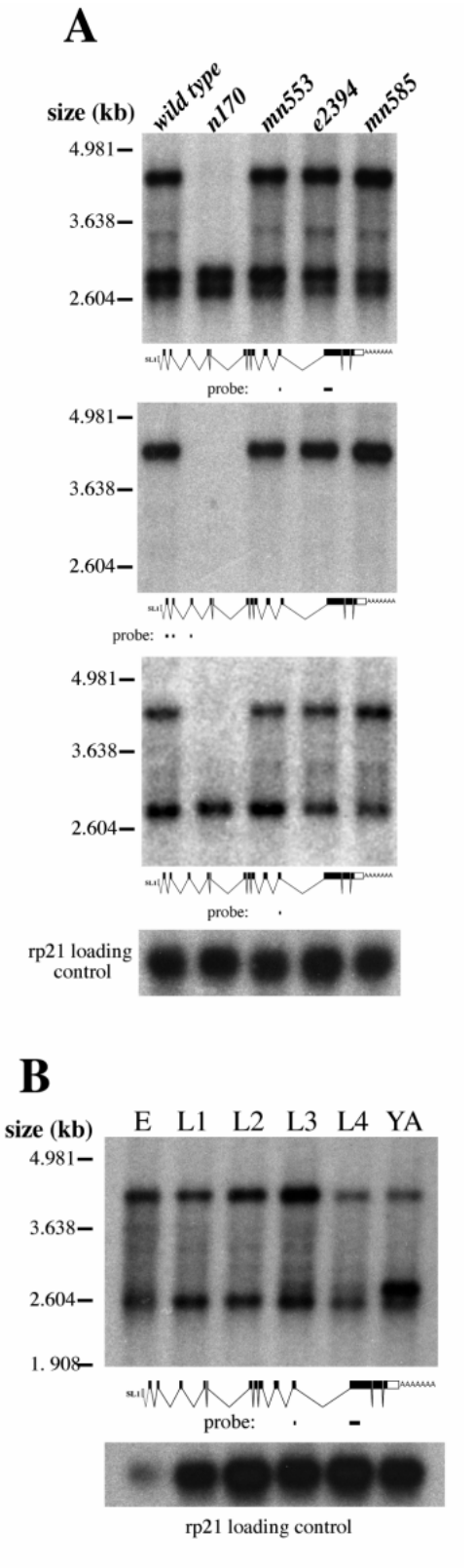

Fig. 5. Northern analysis of *egl-27* transcripts. (A) 2 μg of poly(A)+ RNA from each *egl-27* mutant were probed with different portions of the *egl-27* composite cDNA. Location of the probe used relative to the *egl-27* cDNA is shown below each panel. (Top) 670 bp probe corresponding to bp 1490-2160 of the composite cDNA containing portions of exons 10 and 11. The faint band at approximately 3.5 kb may be a minor transcript or a degradation product of the largest transcript. (Second panel) 363 bp probe corresponding to bp 28-391 of the composite cDNA containing exon 1, exon 2 and a portion of exon 3. (Third panel) 171 bp exon 10 specific probe corresponding to bp 1421-1592 of the composite cDNA. (Bottom) A probe to the ribosomal protein gene rp21 was used as a loading control. (B) 2 μg of staged poly(A)+ RNA from embryos (E), L1, L2, L3, L4 and young adult (YA) wild-type animals was probed with the 670 bp probe that detects all three *egl-27* transcripts (as in the top of A). The faint bands between the 4.3 kb and 2.7 kb bands may be minor transcripts or degradation products of the largest transcript. A probe to rp21 was used as a loading control, but appears to be expressed at lower levels in embryos (T. Starich, personal communication). Sizes of RNA markers run on each blot are shown.

sequence tag (EST) clones (provided by Y. Kohara) and from library screenings to generate the composite cDNA shown in Fig. 4B. We sequenced both strands of the overlapping cDNA clones. One of the 5′ cDNA clones contained a portion of the SL1 trans-spliced leader sequence (Krause and Hirsh, 1987) at its 5′ end, indicating that it is likely to carry the 5′ end of the trans-spliced *egl-27* transcript. The composite *egl-27* cDNA is 4,063 bp long, contains 13 exons, and is derived from a 12,887 bp segment of genomic DNA. The composite cDNA contains a 3387 nt open reading frame, a 61 nt 5′ untranslated region, a 597 nt 3′ untranslated region that includes two sequences, AGTAAA and ATTAAA, which have been shown to function as polyadenylation signals in *C. elegans* (Blumenthal and Steward, 1997), and a poly(A) tail (GenBank accession AF096618).

We found DNA lesions for all four *egl-27* mutations (Fig. 4B). The *n170* mutation is a deletion that removes at least the first eight exons of *egl-27* (data not shown). Each of the other *egl-27* mutations was associated with a C-to-T transition that changed a glutamine residue to a stop codon. The *mn553*, *e2394* and *mn585* lesions are at nucleotides 280, 982 and 2797 of the *egl-27* composite cDNA, respectively, resulting in stop codons in place of amino acid residues 74, 308 and 913 (Fig. 4B,C), respectively. Changes in the coding sequence detected in all four *egl-27* mutants alleles confirmed that we have identified the *egl-27* locus.

EGL-27 contains a domain similar to a metastasis-associated factor

Translation of the *egl-27* composite cDNA yielded a predicted protein of 1129 amino acid residues (Fig. 4C), containing two predicted bipartite nuclear localization signals (Robbins et al., 1991) and a glutamine-rich region at the carboxy terminus. A search of databases revealed that the amino terminus of the predicted *egl-27* protein contains a region of similarity to a metastasis associated factor, Mta1 (Toh et al., 1994). The *mta1* gene showed increased expression in a rat mammary adenocarcinoma metastatic cell line (Pencil et al., 1993). An amino-terminal portion of the putative *egl-27* protein is 23.9% identical to the rat *mta1* product over 641 amino acid residues (aa) of the 703 aa rat protein and is 23.4% identical to the human mta1 product over 607 aa of the 715 aa human *mta1* protein. All three proteins are 24% identical over 438 aa (Fig. 4D).

egl-27 transcripts

Northern analysis using various portions of the composite cDNA as probes on blots of wild-type and *egl-27* mutant mRNAs revealed three major *egl-27* transcripts (Fig. 5A). The

largest, approximately 4.3 kb, corresponds to the composite *egl-27* cDNA and is missing in the *n170* deletion mutant. The two smaller transcripts, 2.8 kb and 2.7 kb, are present in all four mutants and appear to be transcribed from start sites within the *egl-27* transcriptional unit. Because the 2.8 kb and 2.7 kb transcripts are detected in the *n170* deletion mutant and the right endpoint of *n170* breaks after exon 8 and before exon 10, these transcripts must begin after exon 8. The 2.8 kb transcript was detected by probes containing sequences from exons 10 and 11 and from exon 10 alone, but was not detected by probes containing sequences from exons 1-3; this transcript could begin at exon 9 or 10. The 2.7 kb transcript was detected by a probe containing sequences from exons 10 and 11 but not by probes containing either sequences from exons 1-3 or exon 10 alone, suggesting that it begins at exon 11 (Figs 5A, 4B). The lesions associated with mutations *mn553* and *e2394* map to the largest transcript, suggesting that it encodes the EGL-27 protein that functions in cell polarity and cell migration.

We probed a developmental northern blot containing mRNAs prepared from staged wild-type animals with a probe that recognizes all three transcripts (Fig. 5B). The 4.3 kb and 2.7 kb transcripts were expressed at all stages. The 2.8 kb transcript was not detected in the embryo, L1 or L2 stages but was detected in the L3 through young adult stages.

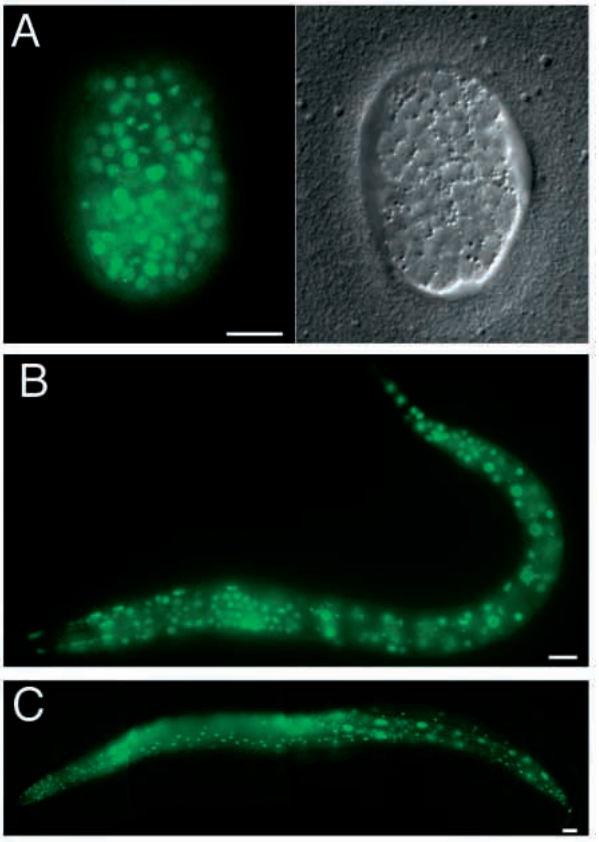

Fig. 6. A functional *egl-27* reporter construct is expressed in all somatic nuclei. GFP expression in *unc-29; mhEx7* animals: (A) ventral view of an approximately 260-minute embryo as viewed with fluorescence (left) and DIC optics (right). (B) L1 stage. (C) Adult. All somatic nuclei appear to express GFP in each animal. The diffuse fluorescence in C is due to autofluorescence of the gut. Bars, 10 μm (A,B) and 50 μm (C).

EGL-27 is expressed in all somatic nuclei throughout development

A transgene in which the Green Fluorescent Protein (*gfp*) (Chalfie et al., 1994) was fused in-frame with *egl-27* and whose expression was designed to be driven by the *egl-27* promoter rescued the T cell polarity defects of *egl-27(mn553)* and *egl-27(n170)* mutants. This construct begins 2046 bp upstream of exon 1, places the *gfp* tag at the end of the *egl-27* coding region, and is likely to tag proteins made from all three *egl-27* transcripts. The construct appeared to be expressed in all somatic nuclei from mid-embryogenesis through adulthood (Fig. 6). A construct which begins 415 bp upstream of exon 1 rescued *egl-27* mutants only poorly and was expressed in the same pattern as the fully rescuing construct. Possibly the two smaller *egl-27* transcripts are responsible for most of the expression we have observed.

egl-27 functions within the T cells to control cell polarity

Mutations in *egl-27* result in a loss of T cell polarity, whereas mutations in *lin-44* result in the reversal of T cell polarity. We analyzed genetic mosaics to see if *egl-27*, in contrast to *lin-44*, affects T cell polarity cell autonomously. To generate *egl-27* mosaics, we made *unc-29; egl-27* animals transgenic for an extrachromosomal array of DNA that contains the functional *egl-27::gfp* fusion and a wild-type copy of *unc-29*. The extrachromosomal array, *mhEx7*, is subject to mitotic loss, which produces a clone of mutant cells. Since the *egl-27::gfp* fusion expresses GFP in all somatic nuclei, we used GFP expression to track the cell-by-cell transmission of *mhEx7*.

The T cells are descendants of AB.p, the posterior daughter of AB, and *unc-29* acts among the descendants of P_1 (AB and P_1 are products of the first embryonic division). We scored non-Unc-29 animals for the polarity of each T cell and then determined whether or not the T cells were GFP positive and hence carried the array. When the array was missing from the T cell descendants, we scored a representative set of cells from all parts of the lineage to determine at which division the array was lost. We found 30 examples in which the polarity of the T cell was abnormal, and in 29 of these, the transgene was missing from the T cell descendants. By contrast, we found 242 examples of normal T cell polarity, and all 242 contained the transgene. We conclude that *egl-27* is required cell autonomously within the T cells for normal polarity.

DISCUSSION

egl-27 mutants are defective in two processes controlled by Wnt signaling

Mutations in *egl-27* cause defects in two processes controlled by two Wnt signals: T cell polarity controlled by LIN-44 and QL.d cell migrations controlled by EGL-20. Mutations affecting other components of the Wnt signaling pathway also cause defects in these processes: mutations in *lin-17* cause defects in T cell polarity and in the migrations of the QL.d cells, and mutations in *bar-1* cause defects in the migrations of QL.d (Harris et al., 1996; Maloof et al., 1998). We have also observed variably abnormal migrations of the HSN, ALM and CAN neurons in *egl-27* mutants similar to those previously observed in *egl-20* and *lin-17*, although the basis for these defects is not clear (Harris et al., 1996). Since EGL-27 is involved in the control of the same

processes as LIN-44 and EGL-20, it must intersect directly or indirectly with these Wnt pathways at some level.

Our results indicate that *egl-27* acts cell-autonomously within the T cell to control its normal polarity, suggesting that *egl-27* acts in a cell that responds to a Wnt signal. The EGL-27 protein could function in, or in conjunction with, Wnt pathways within responding cells. Alternatively, EGL-27 could act either to regulate the expression of Wnt pathway components or as a downstream effector of Wnt signals.

The end result of the transduction of Wnt signals seems to be the activation of a target gene in the nucleus. In *Drosophila*, target genes are *engrailed* in the control of segment polarity and *Ultrabithorax* in the formation of the visceral mesoderm (Thuringer et al., 1993). In axis formation in *Xenopus*, the targets genes appear to be *siamois* and *twin*. All of these target genes encode homeodomain proteins. In fact, the presence of Wnt-responsive sites in the promoters of *Ultrabithorax* and *siamois* that are bound by a complex containing LEF-1/TCF and β-catenin indicate that they are likely to be direct targets of Wnt signaling (Brannon et al., 1997; Riese et al., 1997). Similarly, the expression of the homeodomain protein MAB-5 appears to be the target of the EGL-20 Wnt signal transduction pathway that functions in the control of QL migration. Mutations in the conserved components of the Wnt signaling pathway that function in QL migration all affect the expression of MAB-5 (Harris et al., 1996; Maloof et al., 1998). We have shown that *egl-27* mutations also affect the expression of MAB-5. If the targets of Wnt signaling are conserved, then MAB-5 could be a direct target of the EGL-20/Wnt signal. Such a scenario would suggest that *egl-27* acts in the transduction of Wnt signals or in a parallel pathway that also controls MAB-5 expression. Although our experiments do not define the exact point in these pathways where EGL-27 might function, EGL-27 is nuclearly localized, suggesting that its action might be late.

We note that some of the *egl-27* defects have not been observed in existing Wnt pathway mutants in *C. elegans*. In particular, the defect in the Q/V5 division is unique to *egl-27*. This could imply that EGL-27 also functions outside of Wnt signaling. Alternatively, since additional Wnt homologs are present in the *C. elegans* genome that have not been analyzed for this defect, it is possible that EGL-27 could interact with one or more of these Wnts in the control of the Q/V5 division.

Significance of the Mta1 similarity

The amino-terminal region of EGL-27 is similar to the metastasis-associated factor Mta1 (Toh et al., 1994, 1995). Expression of Mta1 was elevated in human breast cancer metastatic cell lines (Toh et al., 1995), as well as in human colorectal and gastric carcinomas (Toh et al., 1997). The biochemical function of Mta1 is unknown. Interestingly, the founding member of the *Wnt* gene family, *Wnt-1*, was initially isolated as a proto-oncogene activated by insertion of a mouse mammary tumor virus that resulted in murine breast cancer (Nusse and Varmus, 1982). Although the association of Mta1 with metastasis is quite intriguing, its in vivo function is not well understood. Our results implicate a related protein, EGL-27, in the control of cell polarity and cell migrations in *C. elegans*, processes previously shown to be regulated by Wnt signaling. Perhaps Mta1 has a similar function in other organisms.

The *egl-27* locus may encode a multifunctional protein or proteins

The region of Mta1 similarity is restricted to the amino terminus of the larger putative EGL-27 protein. What could be the function of the glutamine-rich carboxy-terminal region of EGL-27? Glutamine-rich protein domains have been implicated in protein-protein interactions (Coustry et al., 1998) and transcriptional activation (Pinto and Lobe, 1996). We find that EGL-27 is localized to the nucleus, suggesting that EGL-27 might function as a transcriptional activator. A protein similar to Mta1, ER1 (early response 1), is encoded in *Xenopus* by a transcript whose expression was increased after FGF was added to animal cap explants and appears to be an early target of FGF signal transduction. Interestingly, ER1 is also localized to the nucleus, and a region of the ER1 protein has been shown to function as a transcriptional activator (Paterno et al., 1997).

We observed three major *egl-27* transcripts, the largest of which appears to encode a protein that plays the major role in the control of cell polarity and cell migration. The functions of the proteins encoded by the smaller transcripts are not clear. Neither of the smaller transcripts contains a significant portion of the Mta1 similarity region, and both consist primarily of the glutamine-rich domain. The *egl-27(mn585)* mutation affects all three transcripts and has defects in addition to cell polarity and cell migration, such as body morphology abnormalities and a failure of the pharynx to attach properly to the mouth (M.A.H, unpublished). Similarly, the *egl-27(we3)* mutation also affects all three transcripts and displays defects in muscle and epidermal cell patterning (F. Solari, A. Bateman and J. Ahringer, unpublished). This suggests that EGL-27 may function in cell adhesions necessary for proper organ attachment; that function may or may not involve Wnt signaling.

Our data suggest that the *egl-27* locus encodes a large multifunctional protein, containing a region of similarity to Mta1 and a glutamine-rich region, which functions primarily in the transduction of Wnt signals involved in the control of cell polarity and cell migration. Since EGL-27 is unique among the Mta1-related proteins, being much larger and containing a glutamine-rich region, it is possible that EGL-27 combines functions of other Mta1-related proteins with a glutamine-rich domain for additional protein interactions or transcriptional activation. Possibly the smaller EGL-27 isoforms containing the glutamine-rich region have additional functions.

EGL-27 is a novel regulator of cell polarity and cell migrations

EGL-27 does not resemble any component of any existing signal transduction pathway. Since *egl-27* mutations affect two processes known to be regulated by Wnt signaling, it is possible that EGL-27 could be a novel component of Wnt pathways. On the other hand, Wnt signals can act in parallel with other signals such as TGF-β or EGF (Jiang and Sternberg, 1998; Riese et al., 1997). Thus EGL-27 could be a component of a known or even novel pathway that functions in parallel to Wnt signals.

We thank F. Solari and J. Ahringer for communication of results prior to publication. We thank Jocelyn Shaw and members of the M. Herman, R. Herman, Shaw and Kenyon laboratories for advice and discussion. We are grateful to Jonathan Hodgkin for *egl-27(e2394)*, Y. Kohara for providing cDNA clones, to A. Fire for the GFP expression vector and to the *C. elegans* Genome Consortium for cosmid clones and genome sequence. Some strains used in this work were provided

by the Caenorhabditis Genetics Center. This work was supported by NIH grants GM22387 to R.H., GM56339-02 to M.H. and GM37053 to C.K. Q.C. was supported by a Howard Hughes Medical Institute Predoctoral Fellowship, the Lucille P. Markey Grant to the Program in Biological Sciences at UC San Francisco and the Herbert Boyer Fund.

REFERENCES

Bhanot, P., Brink, M., Harryman Samos, C., Hsieh, J.-C., Wang, Y., Macke, J. P., Andrew, D., Nathans, J. and Nusse, R. (1996). A new member of the *frizzled* family from *Drosophila* functions as a *Wingless* receptor. *Nature* **382**, 225-230.

Blumenthal, T. and Steward, K. (1997). RNA Processing and Gene Structure. In *C. elegans II* (ed. D. Riddle, T. Blumenthal, B. Meyer and J. Priess), pp. 117-145. Cold Spring Harbor Laboratory Press.

Brannon, M., Gomperts, M., Sumoy, L., Moon, R. T. and Kimelman, D. (1997). A beta-catenin/XTcf-3 complex binds to the siamois promoter to regulate dorsal axis specification in Xenopus. *Genes Dev.* 11, 2359-2370.

Cadigan, K. M. and Nusse, R. (1997). *Wnt* signaling: a common theme in animal development. *Genes Dev.* **11**, 3286-3305.

Chalfie, M., Tu, Y., Euskirchen, G., Ward, W. W. and Prasher, D. C. (1994). Green fluorescent protein as a marker for gene expression. *Science* **263**, 802-805.

Coustry, F., Sinha, S., Maity, S. N. and Crombrugghe, B. (1998). The two activation domains of the CCAAT-binding factor CBF interact with the dTAFII110 component of the *Drosophila* TFIID complex. *Biochem. J.* **331**, 291-297.

Desai, C., Garriga, G., McIntire, S. L. and Horvitz, H. R. (1988). A genetic pathway for the development of the *Caenorhabditis elegans* HSN motor neurons. *Nature* **336**, 638-646.

Eisenmann, D. M., Maloof, J. N., Simske, J. S., Kenyon, C. and Kim, S. K. (1998). The beta-catenin homolog BAR-1 and LET-60 Ras coordinately regulate the Hox gene *lin-39* during *Caenorhabditis elegans* vulval development. *Development* **125**, 3667-3680.

Grunert, S. and St Johnston, D. (1996). RNA localization and the development of asymmetry during Drosophila oogenesis. *Curr. Opin. Genet. Dev.* **6**, 395-402.

Harris, J., Honigberg, L., Robinson, N. and Kenyon, C. (1996). Neuronal cell migration in *C. elegans*: regulation of Hox gene expression and cell position. *Development* **122**, 3117-3131.

Hedgecock, E. M., Culotti, J. G., Hall, D. H. and Stern, B. D. (1987). Genetics of cell and axon migrations in *Caenorhabditis elegans*. *Development* **100**, 365-382.

Herman, M. A. and Horvitz, H. R. (1994). The *Caenorhabditis elegans* gene *lin-44* controls the polarity of asymmetric cell divisions. *Development* **120**, 1035-1047.

Herman, M. A., Vassilieva, L. L., Horvitz, H. R., Shaw, J. E. and Herman, R. K. (1995). The C. elegans gene *lin-44*, which controls the polarity of certain asymmetric cell divisions, encodes a Wnt protein and acts cell nonautonomously. *Cell* **83**, 101-110.

Jiang, L. I. and Sternberg, P. W. (1998). Interactions of EGF, Wnt and HOM-C genes specify the P12 neuroectoblast fate in *C. elegans*. *Development* **125**, 2337-2347.

Kenyon, C. (1986). A gene involved in the development of the posterior body region of C. elegans. *Cell* **46**, 477-487.

Krause, M. and Hirsh, D. (1987). A trans-spliced leader sequence on actin mRNA in C. elegans. *Cell* **49**, 753-761.

Lackner, M. R., Kornfeld, K., Miller, L. M., Horvitz, H. R. and Kim, S. K. (1994). A MAP kinase homolog, *mpk-1*, is involved in *ras*-mediated induction of vulval cell fates in *Caenorhabditis elegans*. *Genes Dev.* **8**, 160-173.

Lin, R., Thompson, S. and Priess, J. R. (1995). *pop-1* encodes an HMG box protein required for the specification of a mesoderm precursor in early C. elegans embryos. *Cell* **83**, 599-609.

Maloof, J. N., Whangbo, J., Harris, J. M., Jongeward, G. D. and Kenyon, C. (1998). A Wnt signaling pathway controls Hox gene expression and neuroblast migration in *C. elegans*. *Development* **126**, 37-49.

Mello, C. C. and Fire, A. (1995). DNA Transformation. In Caenorhabditis elegans: *Modern Biological Analysis of an Organism. Methods in Cell Biology* (ed. H. Epstein and D. Shakes), pp. 452-482. San Diego: Academic Press.

Moon, R. and Kimelman, D. (1998). From cortical rotation to organizer gene expression: toward a molecular explanation of axis specification in *Xenopus*. *BioEssays* **20**, 536-545.

Moon, R. T., Brown, J. D. and Torres, M. (1997). WNTs modulate cell fate and behavior during vertebrate development. *Trends Genet.* **13**, 157-162.

Morin, P. J., Sparks, A. B., Korinek, V., Barker, N., Clevers, H., Vogelstein, B. and Kinzler, K. W. (1997). Activation of beta-catenin-Tcf signaling in colon cancer by mutations in beta-catenin or APC. *Science* **275**, 1787-1790.

Nusse, R. and Varmus, H. E. (1982). Many tumors induced by the mouse mammary tumor virus contain a provirus intergrated in the same region of the host genome. *Cell* **31**, 99-109.

Paterno, G. D., Li, Y., Luchman, H. A., Ryan, P. J. and Gillespie, L. L. (1997). cDNA cloning of a novel, developmentally regulated immediate early gene activated by fibroblast growth factor and encoding a nuclear protein. *J. Biol. Chem.* **272**, 25591-25595.

Pencil, S. D., Toh, Y. and Nicolson, G. L. (1993). Candidate metastasis-associated genes of the rat 13762NF mammary adenocarcinoma. *Breast Cancer Res. Treat.* **25**, 165-174.

Pinto, M. and Lobe, C. G. (1996). Products of the grg (Groucho-related gene) family can dimerize through the amino-terminal Q domain. *J. Biol. Chem.* **271**, 33026-33031.

Riese, J., Yu, X., Munnerlyn, A., Eresh, S., Hsu, S. C., Grosschedl, R. and Bienz, M. (1997). LEF-1, a nuclear factor coordinating signaling inputs from *wingless* and *decapentaplegic*. *Cell* **88**, 777-787.

Robbins, J., Dilworth, S. M., Laskey, R. A. and Dingwall, C. (1991). Two interdependent basic domains in nucleoplasmin nuclear targeting sequence: identification of a class of bipartite nuclear targeting sequence. *Cell* **64**, 615-623.

Rocheleau, C. E., Downs, W. D., Lin, R., Wittmann, C., Bei, Y., Cha, Y. H., Ali, M., Priess, J. R. and Mello, C. C. (1997). Wnt signaling and an APC-related gene specify endoderm in early C. elegans embryos. *Cell* **90**, 707-716.

Rubinfeld, B., Robbins, P., El-Gamil, M., Albert, I., Porfiri, E. and Polakis, P. (1997). Stabilization of beta-catenin by genetic defects in melanoma cell lines. *Science* **275**, 1790-1792.

Salser, S. J. and Kenyon, C. (1992). Activation of a *C. elegans Antennapedia* homologue in migrating cells controls their direction of migration. *Nature* **355**, 255-258.

Salser, S. J. and Kenyon, C. (1996). A *C. elegans* Hox gene switches on, off, on and off again to regulate proliferation, differentiation and morphogenesis. *Development* **122**, 1651-1661.

Salser, S. J., Loer, C. M. and Kenyon, C. (1993). Multiple HOM-C gene interactions specify cell fates in the nematode central nervous system. *Genes Dev.* **7**, 1714-1724.

Sambrook, J., Fritsch, E. F. and Maniatis, T. (1989). *Molecular Cloning: A Laboratory Manual*, Second Edition. Cold Spring Harbor, NY: Cold Spring Harbor Laboratory.

Sawa, H., Lobel, L. and Horvitz, H. R. (1996). The *Caenorhabditis elegans* gene *lin-17*, which is required for certain asymmetric cell divisions, encodes a putative seven-transmembrane protein similar to the *Drosophila frizzled* protein. *Genes Dev.* **10**, 2189-2197.

Sternberg, P. W. and Horvitz, H. R. (1988). *lin-17* mutations of *Caenorhabditis elegans* disrupt certain asymmetric cell divisions. *Dev. Biol.* **130**, 67-73.

Sulston, J. and Hodgkin, J. (1988). Methods. In *The Nematode* Caenorhabditis elegans, vol. 1 (ed. W. B. Wood), pp. 587-606. Cold Spring Harbor, NY: Cold Spring Harbor Laboratory.

Sulston, J. E. and Horvitz, H. R. (1977). Post-embryonic cell lineages of the nematode, *Caenorhabditis elegans*. *Dev. Biol.* **56**, 110-156.

Thorpe, C. J., Schlesinger, A., Carter, J. C. and Bowerman, B. (1997). Wnt signaling polarizes an early C. elegans blastomere to distinguish endoderm from mesoderm. *Cell* **90**, 695-705.

Thuringer, F., Cohen, S. M. and Bienz, M. (1993). Dissection of an indirect autoregulatory response of a homeotic *Drosophila* gene. *EMBO J.* **12**, 2419-2430.

Toh, Y., Oki, E., Oda, S., Tokunaga, E., Ohno, S., Maehara, Y., Nicolson, G. L. and Sugimachi, K. (1997). Overexpression of the MTA1 gene in gastrointestinal carcinomas: correlation with invasion and metastasis. *Int. J. Cancer* **74**, 459-463.

Toh, Y., Pencil, S. D. and Nicolson, G. L. (1994). A novel candidate metastasis-associated gene, mta1, differentially expressed in highly metastatic mammary adenocarcinoma cell lines. cDNA cloning, expression, and protein analyses. *J. Biol. Chem.* **269**, 22958-22963.

Toh, Y., Pencil, S. D. and Nicolson, G. L. (1995). Analysis of the complete sequence of the novel metastasis-associated candidate gene, *mta1*, differentially expressed in mammary adenocarcinoma and breast cancer cell lines. *Gene* **159**, 97-104.

Trent, C., Tsung, N. and Horvitz, H. R. (1983). Egg-laying defective mutants of the nematode *Caenorhabditis elegans*. *Genetics* **104**, 619-647.